

# DISPERSION COEFFICIENTS OF SUPERCRITICAL FLUID IN FIXED BEDS

S. M. Ghoreishi

Department of Chemical Engineering, Isfahan University of Technology  
Isfahan 84154, Iran

A. Akgerman

Department of Chemical Engineering, Texas A&M University  
College Station, TX 77843, USA

(Received: December 29, 1997 - Accepted: December 5, 1998)

**Abstract** The axial dispersion coefficient of hexachlorobenzene in supercritical carbon dioxide is investigated in a fixed-bed packed with glass beads. The on-line chromatographic pulse-response experiment is used in order to study the dynamics of a packed column under supercritical conditions. The radial dispersion is assumed negligible because of the packed column geometry. To estimate the axial dispersion coefficient, a pulse input of tracer/supercritical fluid (hexachlorobenzene/carbon dioxide) mixture is injected into the column and the effluent peak is analyzed using the moments of the chromatographic curve in the Laplace domain. The range of the operating conditions for temperature, pressure and flow rate of supercritical fluid are 25-500°C, 200-4000 psia and 20-160 ml/hr, respectively. The experimental data indicate that the axial dispersion coefficient is a function of temperature, pressure and flow rate. The axial dispersion coefficient decrease with increasing temperature and increase with increasing pressure. This trend may be due to the increase of the density and viscosity of the supercritical carbon dioxide. Furthermore, the axial dispersion coefficient increase with increasing interstitial velocity. These results suggest that the contribution by convection is more important than molecular diffusion under supercritical operations. In order to investigate the authenticity of the dynamic model as well as the extent of accuracy of the moment analysis which is used for parameter estimation, the experimental response peak is compared with the dimensionless theoretical (numerical solution) curve. The small deviation between the two curves is well within the range of experimental error of axial dispersion coefficient measurements.

**Key Words** Supercritical Fluid, Axial Dispersion Coefficient, Carbon Dioxide, Glass Beads

RAI pAK @oTM 1/2 j » AdM ±SS lK k A j rj -q%2- qcu° n d«» fK @CK k t k h a  
-±Tw0 k 2 3 i S v x° B w n j ° A { d S } S e H B o » μ B z B p C x ° n p A S S e n a 3 i S v j n e «° A z ¼  
n A C d k C » i B C » f K @ C Q k @ e ± T v » v k p j B M M j ± U B M { 3 B T A » A d M ± S v ¼ n j 7 k @  
° -q M i G a C p » C a d M ± S e B w J B y n p » x ± h «, ° n d «» f K @ C K k t S h U A M S S C  
» @ Q ° n B C B p -i B p j B T A B M ± T w p » ] ° d n A ± ° k { C e n u b M M j ° n 3 M S l K k A e j  
< ± S e B A » M r B S B j ° A v l B A i v ¼ j ° k d « k j o f w o v M t A Q 3 Q A r j » S e H B o @  
7 { S ¼ A S i B v n j o b ! ¼ 1 6 a » 8 1 2 a ° □ 4 a a a » 8 1 2 a a j a c 7 e v j r j 5 a » 8 2 5 K ¼ U P M A d M  
y ¼ S B M - K ¼ U S K M H M M r B S B j 3 V i n d «» f K @ C K k t » C T M M ° B 4 e μ B z B p C ¼ j ± M  
S i C 3 Q M A T G R A ¼ U S A - k { j B e - C A k n B S y ¼ S B M 3 T B y μ B ° n d «» f K @ C K k t B j  
r j » C a d M ± S e B A S i o w y ¼ S A - C o M A i k { B v A d M ± S S l K k A e j » f K @ v a ° » S e a y ¼ S A  
» B i B i q 7 e « O z ¼ U U U B 4 e S w S n ° « [ B S ¼ k j o f S x » f K @ C A ¼ k { j B o M B k @ o T M  
° » n ¼ 2 d k « n B T A » w o v M M k { B v A d M ± S » B 4 i v ¼ n j » S n S « l ± % B v M B k r j 3 v B k r j  
» @ Q j ± K { 3 S e r B M d j n e « k A B S 7 h U A v l ° n B C q S C ° n Y a i S j - A ¼ 3 i S v S ¼ a μ  
° B v C S i C 3 Q M A T k » @ Q ° j S ¼ A B † A T A 3 - k { 3 v B k ° n A ¼ B » @ Q B v μ B z B p C ¼ B  
k { B v n d «» f K @ C K k t ° o ¼ K A μ B z B p C

## INTRODUCTION

In recent years, there has been an increasing interest in supercritical fluids (SCF) resulting

from potential applications in chemical, petrochemical, pharmaceutical, environmental, food and synfuels processes, improved

separation methods and as non-toxic, non-carcinogenic solvents [1-9]. In order to use supercritical fluids in a large scale system, the relevant dynamic packed column parameters such as the dispersion coefficient under supercritical conditions should be investigated. Although certain supercritical fluid processes are already commercialized, fundamental data on the dispersion coefficient and its dependence upon the fluid physical properties, operation variables and the fixed bed geometry are lacking.

Axial dispersion of a gas or a liquid has been the subject of many investigations. Levenspiel and Smith [10] studied the longitudinal dispersion coefficient in terms of the dimensionless Peclet number. The radial and axial dispersions of gas and liquid were studied in packed and fluidized beds and some approximate relationships between the Peclet group and the Reynolds and Schmidt numbers were presented [11-23]. Westerterp et al. [24] proposed a new 1-D wave model for longitudinal dispersion as an alternative to the Fickian-type dispersed plug-flow model. The axial dispersion in Taylor-Couette flow was studied and a correlation of Peclet number as a function of Reynolds number for short and long cylinders was developed [25]. Kohav et al. [26] investigated axial dispersion of solid particles in a continuous rotary kiln.

Even though the behavior of a supercritical fluid lies between those of a gas and a liquid, the interpolation of dispersion coefficients between gas and liquid for supercritical conditions is questionable. Tan and Liou [27] measured the axial dispersion coefficients under supercritical operations by injection of a pulse of methane in supercritical carbon dioxide. They correlated the dependence of the axial dispersion upon the Reynolds and Schmidt numbers, through which it was found that the

correlations in terms of the Peclet, Reynolds, and Schmidt dimensionless groups did not offer satisfactory prediction. Lee and Holder [28] used toluene and naphthalene in supercritical carbon dioxide in silica gel packed beds to generalize a mass transfer correlation which considers both the effects of natural and forced convection and the effect of axial dispersion at  $0.3 < Re < 135$ .

There is not much information on the dispersion at supercritical conditions in the literature. Therefore, the main objective of this research was to experimentally measure the axial dispersion under supercritical operation and to investigate whether factors influencing axial dispersion for gases and liquids offer similar effects on axial dispersion of a supercritical fluid.

## EXPERIMENTAL APPARATUS AND PROCEDURE

**A. Apparatus** In order to carry out this study, the dynamic system shown in Figure 1 is used. This system operates at a temperature range of 25-50°C with a maximum pressure of 7500 psia. The system is constructed so that any non-corrosive gas can be used as the supercritical fluid. The experimental set-up consists of the following: (1) nitrogen gas cylinder, (2) carbon dioxide gas cylinder, (3) valve (model 10V-4073, Autoclave Engineers), (4) piston cylinder (model 10V-4073, Autoclave Engineers), (7) preheater (Swagelok), (8) injection valve (model 7000, Rheodyne Inc.), (9) constant temperature circulator (model 70, Fisher Scientific), (10) valve (model 10V-4073, Autoclave Engineers), (11) saturator column (model CNLX 1608, Autoclave Engineers), (12) packed column (model CNLX 1608, Autoclave Engineers), (13) pressure gauge (model BU-2581-AM, USG), (14) valve (model 10V-4073, Autoclave Engineers), (15) computer terminal (model IBM XT compatible clone,

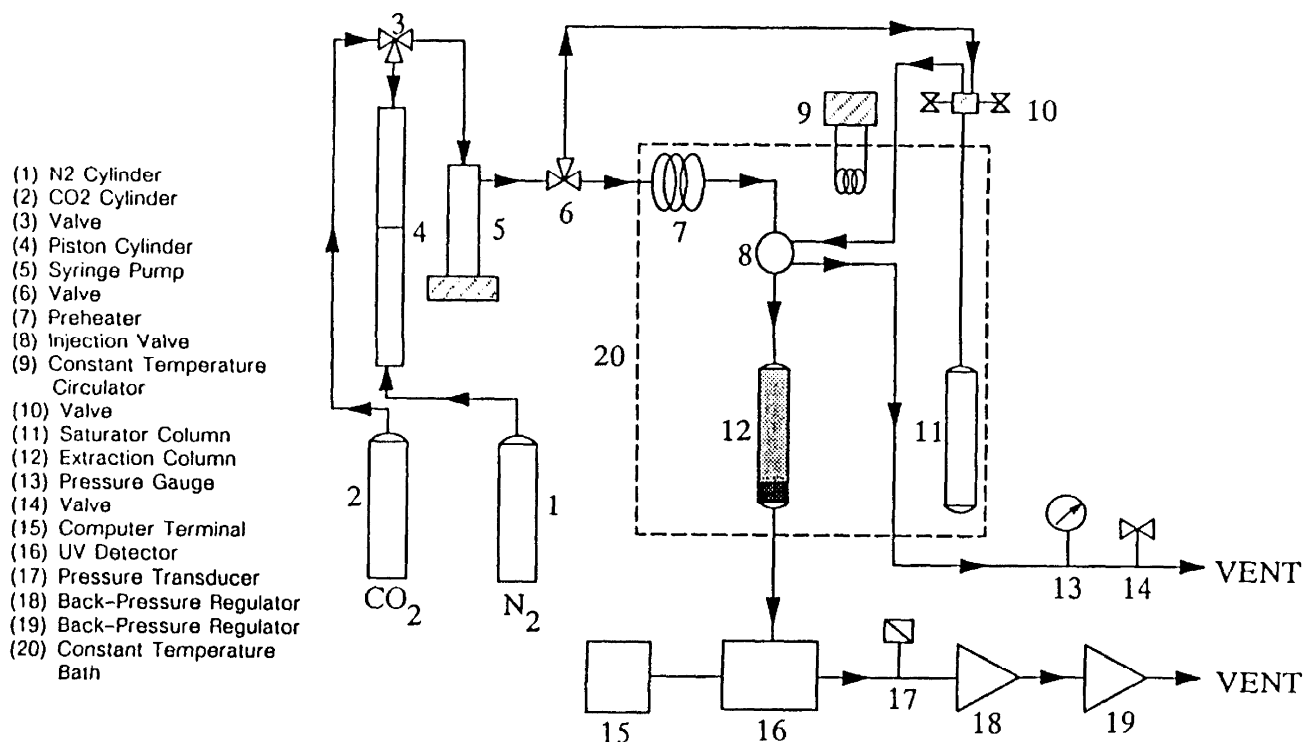


Figure 1. The experimental set-up for the supercritical extractor system.

Samsung), (16) supercritical monitor high pressure UV detector, Milton Roy), (17) pressure transducer (model A 006220 Th-1V, Hydronics), (18 and 19) back pressure regulators (model 26-1722-24, Tescom Inc.), (20) constant temperature bath. The syringe pump operates in a constant flow mode and has a digital display of pressure in psi or Mpa. The syringe barrel and piston are made of 303 stainless steel which is more resistant to corrosive solvents and halogen acids. The pump is designed for applications requiring accurate, pulse free delivery of liquids. Figure 2 shows the detailed description of the packed column. As shown in Figure 2, the column is packed with glass beads with particle diameter of 0.1 cm and bed porosity of 39% (Thomas Scientific LTD, catalog no. 5663-R70) and a porous metal filter (model 1003630-01-050, Mott Metallurgical Corp.) with a porosity of 0.5 micron is placed at the bottom of the column. This is done to prevent the movement of solid particles out of

the packed column which subsequently may plug the system and cause a safety problem. The critical extraction monitor used in this study is a continuously variable wavelength UV-visible spectrophotometer designed for entrained solute measurement in supercritical process studies. It is equipped with a high pressure fluid cell (5000 psi at 60°C maximum allowable working pressure) to detect and quantify entrained organic compound extracts.

**B. Procedure** To measure the axial dispersion coefficient for HCB in supercritical carbon dioxide, the following steps were followed. First, the extraction column was filled with glass beads. Initially, the syringe pump (5) was empty and fully retracted. The piston cylinder (4) was charged with liquid carbon dioxide (850 psia). The carbon dioxide in the piston cylinder was then compressed using high pressure nitrogen in order to fill the syringe pump with liquid carbon dioxide. The syringe pump was then isolated

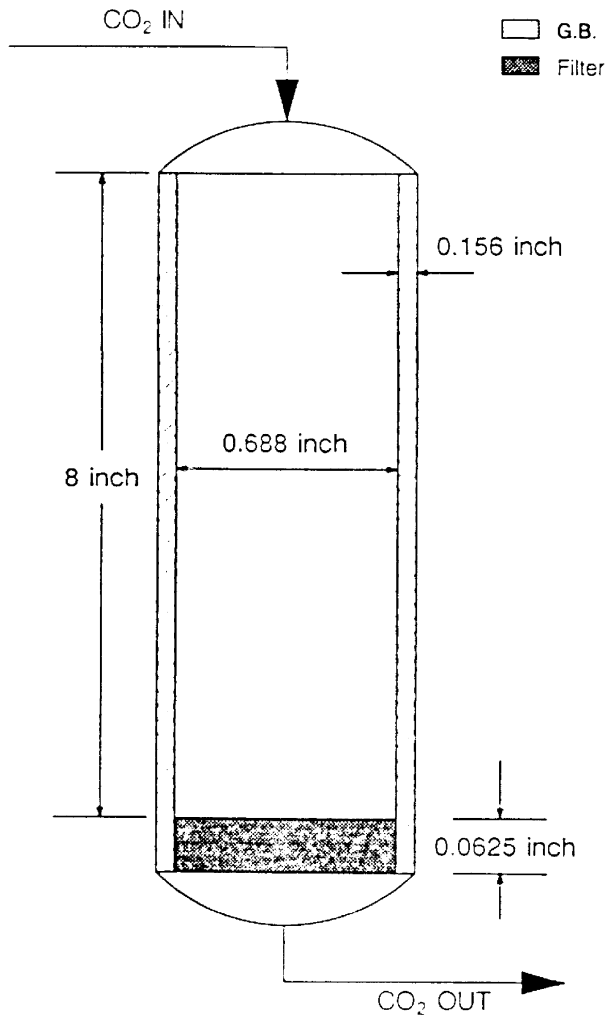


Figure 2. Description of extraction column.

through the shut off valve. The syringe pump was later used to pump the carbon dioxide through the system at the desired flow rate. Next, one gram of standard hexachlorobenzene (not  $^{14}\text{C}$  labeled HCB) as the tracer compound was placed in the saturator column (11) and then high pressure carbon dioxide was fed to the saturator column in order to dissolve the hexachlorobenzene. The pressure in the saturator column was monitored by the pressure gauge (13). Using the syringe pump, the high pressure carbon dioxide was continuously passed through the packed bed while its pressure and flow rate were monitored with the

pressure transducer (17) and the syringe pump. The pressure in the system was maintained with the back-pressure regulators (18 and 19). The temperature of the supercritical fluid was controlled by the constant temperature circulator (9) which was placed inside the constant temperature bath (ethylene glycol bath,  $0-90^\circ\text{C}$ ). Then using the injection valve (8), a square pulse of tracer/supercritical fluid (hexachlorobenzene/carbon dioxide) mixture from the saturator column was introduced into the fixed bed filled with glass beads. The outlet stream from the packed bed was passed through a high pressure critical extraction monitor (UV detector) (16) which was connected to a computer terminal (15). The response peak to the pulse input of hexachlorobenzene/carbon dioxide mixture was recorded as volts versus time. By analyzing this response curve by the moments of the chromatographic peak, the axial dispersion coefficient was determined for different operating conditions for the supercritical fluid (pressure, temperature and flow rate).

## MATHEMATICAL MODELING AND PARAMETER ESTIMATION

The system in the packed column consists of the glass beads, the supercritical fluid (carbon dioxide)  $R$  and the tracer compound (hexachlorobenzene). In this study, a one phase (mobile) model is considered and the induced convection and dispersion are the significant transport processes responsible for tracer migration. The dynamic behavior of a supercritical fluid system such as the packed column, as described above, may be classified according to the nature of the mathematical model required to describe the system. The complexity of the mathematical model depends on the concentration level, heat transfer effect,

and the choice of flow model. In this research, the following criteria are assumed. (1) Trace systems. The traceable component is present only at low concentration in an inert carrier. Changes in fluid velocity across the mass transfer zone are therefore negligible. Furthermore, it is assumed that radial concentration gradients do not exist. (2) Isothermal fixed bed. Heat transfer resistance can be neglected. The spreading of the concentration front is due entirely to the axial dispersion and bulk flow effects. This is the usual situation in a chromatographic system in which the traceable component is present only at low concentration in an inert carrier (carbon dioxide). (3) Dispersed plug flow. Axial dispersion is significant and it must be included in the mathematical model in contrast to the radial dispersion which can be neglected because of the packed bed geometry (small column diameter). Thus, a one-dimensional, unsteady-state dispersion model is considered and the pressure drop through the packed bed is neglected.

#### A. MATHEMATICAL MODEL OF AN ISOTHERMAL PACKED COLUMN

For the described model, the concentration of the traceable component as a function of axial position and time in the bed can be expressed by the mass balance of the solute in the mobile phase. Since the solute (HCB) is transported through the differential column element by both axial dispersion and convection, the mass balance for the mobile phase becomes:

$$D_z \frac{\tilde{A}^2 C_A}{\tilde{A} Z^2} - \frac{Q}{e_z A_c} \frac{\tilde{A} C_A}{\tilde{A} Z} = \frac{\tilde{A} C_A}{\tilde{A} t} \quad (1)$$

The parameter of interest that needs to be determined in equation (1) is the axial dispersion coefficient ( $D_z$ ). In studying the dynamics of a fixed-bed column it is convenient

to consider the response of an initially tracer free column to the injection of a small pulse of tracer at the column inlet (pulse input). The response to a pulse input is often referred to as the chromatographic response. In this project, a pulse input of HCB/CO<sub>2</sub> mixture is introduced at the inlet plane into the supercritical carbon dioxide flowing over a glass beads matrix. The boundaries of the packed column are taken here as closed for dispersion at the inlet and outlet of the column. At the inlet of the fixed bed there is a square pulse input of tracer (HCB). Therefore, the first boundary condition for this system is given by:

$$\text{at } Z=0 ; C_A = 0 \text{ for } t < 0 \text{ \& } t > t \text{ and } C_A = C_{A0} \text{ for } 0 \leq t \leq t \text{ (injection time)} \quad (2)$$

At the outlet the second boundary condition is :

$$\text{at } Z = L ; \frac{\tilde{A} C_A}{\tilde{A} Z} = 0 \quad (3)$$

This boundary condition can be understood by realizing that no dispersion flux is assumed to occur through the plane  $Z=L$  and continuity in tracer concentration of mobile phase is to be expected on both sides of the plane at  $Z=L$ .

#### B. PARAMETER ESTIMATION SOLUTION IN THE LAPLACE DOMAIN

In this study, the moment analysis is used to determine the model parameter. The purpose of this approach is to obtain a solution for the chromatographic curve in the Laplace domain which includes the effect of the axial dispersion coefficient. This solution is then used to relate moments of the chromatographic curve to the dynamic parameter. First, the equation for the mobile phase (equation 1) along with the boundary conditions (2) and (3) are transformed to the Laplace domain.

$$\left[ D_z \frac{\tilde{A}^2 C_A^*}{\tilde{A} Z^2} \right] - \left[ \frac{Q}{e_z A_c} \frac{\tilde{A} C_A^*}{\tilde{A} Z} \right] = S C_A^* \quad (4)$$

$$\text{at } Z=0; C_A^* = \left[ \frac{C_{A0}}{S} \right] [1 - \exp(-st)] \quad (5)$$

$$\text{at } Z=L; \frac{\tilde{A}C_A^*}{\tilde{A}Z} = 0 \quad (6)$$

By applying the boundary conditions (5) and (6), the solution for equation (4) in the Laplace domain is obtained:

$$C_A^* = \left[ \frac{C_{A0}}{S} \right] [1 - \exp(-st)] [\exp(r_2 z)] \quad (7)$$

where

$$r_2 = \left[ \frac{Q}{2e_z A_c D_z} \right] - \left[ \frac{1}{2} \left\{ \left[ \frac{Q}{e_z A_c D_z} \right]^2 + 4 \hat{E} \right\} \right]^{1/2} \quad (8)$$

$$\hat{E} = \left[ \frac{S}{D_z} \right] \quad (9)$$

### C. MOMENTS OF THE CHROMATOGRAPHIC CURVE

The moments of the chromatographic peak leaving the fixed-bed column are related to the solution in the Laplace domain by the expression [29]:

$$m_n = (-1)^n \lim_{s \rightarrow 0} \left[ \frac{\tilde{A}^n C_A^*}{\tilde{A} s^n} \right] \quad (10)$$

where

$$m_n = \beta C_A t^n dt \quad (11)$$

Then the n-th absolute and central moments [23] are given in equations (12) and (13), respectively:

$$m_n = \frac{m_n}{m_0} = \frac{\beta C_A t^n dt}{\beta C_A dt} \quad (12)$$

$$m_n^{\Delta} = \frac{\beta C_A (t - \bar{m})^n dt}{\beta C_A dt} = \sum_{j=0}^n \tilde{\omega} (-1)^{n-j} \left[ \begin{matrix} n \\ j \end{matrix} \right] m_j m^{n-j} \quad (13)$$

By applying equations (10), (12) and (13) to the solution in the Laplace domain (equation 7), the zeroth, first and second moments are derived analytically. The zeroth reduced moment is :

$$m_0 = \frac{m_0}{(m_0)_{Z=0}} = \frac{C_{A0} t}{C_{A0} t} = 1 \quad (14)$$

where  $m_0$  is the measure of the total amount of tracer in the effluent response peak and  $(m_0)_{Z=0}$  is the measure of the total amount of tracer in the pulse input. The first absolute moment is :

$$m_1 - \frac{t}{2} = \left[ \frac{L e_z A_c}{Q} \right] \quad (15)$$

The second absolute moment is :

$$m_2 - \frac{t^2}{3} = (t) \left[ \frac{L e_z A_c}{Q} \right] + [2D_z L] \left[ \frac{e_z A_c}{Q} \right]^3 + \left[ \frac{L e_z A_c}{Q} \right]^2 \quad (16)$$

The second central moment is :

$$m_2^{\Delta} - \frac{t^2}{12} = [2] \left[ \frac{L A_c e_z}{Q} \right]^2 \left[ \frac{D_z A_c e_z}{L Q} \right] \quad (17)$$

By assuming an instantaneous injection of tracer (where the injection time,  $t$ , is assumed to be zero) into the fluid which is moving down the packed bed at  $Z=0$ , equation (17) in conjunction with equation (15) reduces to :

$$\frac{m_2^{\Delta}}{m_1^2} = \left[ \frac{D_z e_z A_c}{L Q} \right] \quad (18)$$

The first absolute moment and the second central moment of the chromatographic peak are calculated directly from the experimental data using finite summation by the following equations:

$$m_1 = \frac{\tilde{\omega} t_i c_i D t_i}{\tilde{\omega} c_i D t_i} \quad (19)$$

$$m_2^{\Delta} = \frac{\tilde{\omega} t_i^2 c_i D t_i}{\tilde{\omega} c_i D t_i} - m_1^2 \quad (20)$$

Finally, substituting a value for the experimental first absolute moment ( $m_1$ ) and the experimental second central moment ( $m_2^{\Delta}$ ) in equation (18) results in one equation and one unknown which is solved for the axial dispersion coefficient.

### D. NUMERICAL SOLUTION

In order to demonstrate the authenticity of the dynamic model and also to investigate the extent of accuracy of the moment analysis which

is used for parameter estimation, the comparison of the experimental response peak to the dimensionless theoretical curve is necessary. To obtain a numerical solution, first a value for DZ obtained from moment analysis is substituted in equation (1) and then this equation along with the two boundary conditions (2) and (3) are transformed into a dimensionless form by rewriting them in terms of the following dimensionless variables:

$$X = \frac{Z}{L}, \quad C_A^{**} = \frac{C_A}{C_{A0}}, \quad q = \frac{tu}{L} = \frac{t}{j},$$

$$Pec = \frac{LQ}{e_z A_c D_z} \quad (21)$$

Thus, the following dimensionless equations for the mobile phase and the boundary conditions are obtained:

$$\left[ \frac{1}{Pec} \frac{\bar{A}^2 C_A^{**}}{\bar{A}_x^2} \right] - \left[ \frac{\bar{A} C_A^{**}}{\bar{A}_x} \right] = \frac{\bar{A} C_A^{**}}{\bar{A} q} \quad (22)$$

$$\text{at } x=0; \quad C_A^{**} = 0 \text{ for } q < 0 \text{ and } q > \frac{t}{j} \quad (23)$$

$$C_A^{**} = 1 \text{ for } 0 \leq q \leq \frac{t}{j}$$

$$\text{at } x = 1; \quad \frac{\bar{A} C_A^{**}}{\bar{A}_x} = 0 \quad (24)$$

Using the method of lines (MOL), equation (22) along with the boundary conditions (23) and (24) is solved numerically to obtain a theoretical response curve for the glass beads experiments. In the method of lines solution of a PDE problem, the dimensionless spatial coordinate (x-axis) is discretized and the spatial derivatives are obtained from five-point, fourth-order central finite difference approximations. This procedure results in a system of ordinary differential equations (ODEs) which can be integrated using an IMSL LIBRARY routine called DIVPAG that is based on Gear's method. This FORTRAN program generates a theoretical response curve

in terms of the concentration of tracer in the mobile phase ( $C_A^{**}$ ) versus time ( $q$ ). These theoretical response curves are then compared with the experimental response peaks to investigate the validity of our dynamic model and also to investigate the accuracy of the experimental measurements.

## E. PROPAGATION OF RANDOM ERROR

Once the final result for an experiment is calculated, the investigator is faced with the task of determining the uncertainty to which the experimental result is subject. Let the desired result, for which the experiment was carried out, be designated by F and let the directly measured quantities be designated by x, y and z. The value of F is determined by substituting the experimentally determined values of x, y and z into a formula:

$$F = f(x, y, z) \quad (25)$$

Obviously errors in x, y and z produce an error in F,

$$DF = e(F) = F(\text{Calculated by measured } x) - F(\text{true}) \quad (26)$$

the value of which is given by :

$$e(F) = \frac{\bar{A}_F}{\bar{A}_x} e(x) + \frac{\bar{A}_F}{\bar{A}_y} e(y) + \frac{\bar{A}_F}{\bar{A}_z} e(z) \quad (27)$$

In the case of random errors, the actual values of  $e(x)$ ,  $e(y)$  and  $e(z)$  are not known and the actual value of  $e(F)$  can not be determined. But it is possible to determine error in terms of the variance and subsequently the standard deviation of F. Thus, the variance in F using Taylor series expansion is given by :

$$[e(F)]^2 = \left[ \frac{\bar{A}_F}{\bar{A}_x} \right]^2 [e(x)]^2 + \left[ \frac{\bar{A}_F}{\bar{A}_y} \right]^2 [e(y)]^2 + \left[ \frac{\bar{A}_F}{\bar{A}_z} \right]^2 [e(z)]^2 \quad (28)$$

In this study, we had +/- 0.5% uncertainty in the flow rate and our reproducibility in the first and second moments were +/- 0.8% and +/- 2.1%, respectively. The axial dispersion coefficient was estimated from the following equation:

$$D_z = \left(\frac{m_2 \dot{A}}{m^2}\right) \left(\frac{LQ}{2 e_z A_c}\right) \quad (29)$$

where

$$D_z = f(Q, m, m_2 \dot{A}), \quad m = f(Q), \quad \text{and} \quad m_2 \dot{A} = f(Q)$$

By applying equation (28) to equation (29), we determined how the error in flow rate affected the end result for the axial dispersion coefficient:

$$[e(D_z)]^2 = \left\{ \left(\frac{m_2 \dot{A}}{m^2}\right) \left(\frac{L}{2 e_z A_c}\right) \right\}^2 [e(Q)]^2 + \left\{ -\left(\frac{m_2 \dot{A}}{m^3}\right) \left(\frac{LQ}{e_z A_c}\right) \right\}^2 [e(m)]^2 + \left\{ \left(\frac{1}{m^2}\right) \left(\frac{LQ}{2 e_z A_c}\right) \right\}^2 [e(m_2 \dot{A})]^2 \quad (30)$$

By Substituting  $e(m)$ ,  $e(m_2 \dot{A})$  and  $e(Q)$  in the above equation, the error in the axial dispersion coefficient as +/- one standard deviation was determined.

## RESULTS AND DISCUSSIONS

To study axial dispersion in a packed bed experimentally, by using glass beads we eliminated the adsorption/desorption effect from the extraction process which subsequently resulted in only one parameter, namely, the axial dispersion coefficient. The response curves obtained in the glass beads experiments were very sharp and they contained no tailing at the end of the peak. In this study, the following operating variables were varied to observe their effects on the axial dispersion coefficient: pressure, temperature and flow rate.

### A. TEMPERATURE AND PRESSURE EXPERIMENTS

To investigate the behavior of the axial

dispersion coefficient as a function of temperature and pressure of the extracting fluid (carbon dioxide), three different series of experiments were carried out. In the first series, the temperature was held constant at 298 K while the pressure was varied from 1.2 kpsia to 4.0 kpsia. In the second series of experiments, the temperature was increased to 308 K and held constant while the pressure of the extracting fluid was varied from 2.5 kpsia to 4.0 kpsia. The third series of experiments determined how the axial dispersion coefficient varied as a function of pressure (from 2.5 kpsia to 4.0 kpsia) at 323 K. The flow rate of carbon dioxide was held constant at 160 mL/hr for all three series of experiments. The results of the temperature and pressure experiments of the axial dispersion coefficient are shown in Figure 3. Each data point is the average of at least three independent measurements with +/- 8.6% standard deviation obtained from the propagation of errors.

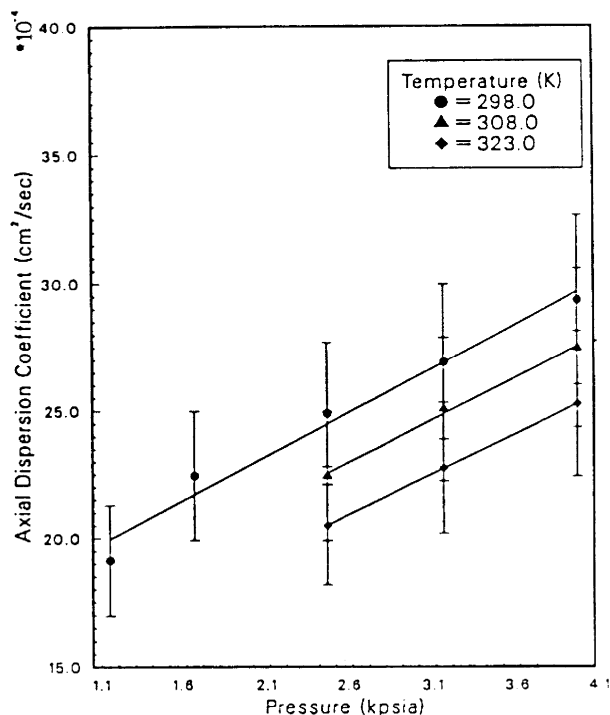


Figure 3. The effect of temperature and pressure of CO<sub>2</sub> on the axial dispersion coefficient.



TABLE 1. The Density and Viscosity of Carbon Dioxide at Different Temperatures and Pressures.

(P,kpsia)	298 K		308 K		323 K	
	Density	Viscosity	Density	Viscosity	Density	Viscosity
1.2	0.780	628.0	—	—	—	—
1.7	0.850	726.0	—	—	—	—
2.5	0.895	801.0	0.840	744.0	0.760	715.0
3.2	0.927	867.0	0.890	824.0	0.810	780.0
4.0	0.950	913.0	0.920	900.0	0.860	855.0
Density =g/cm <sup>3</sup>		Viscosity= [g/(cm.sec)] (10 <sup>6</sup> )				

At the temperature of 298 K, the axial dispersion coefficient was increased by 34.1% as the pressure of the extracting fluid was increased from 1.2 to 4.0 kpsia. At the temperatures of 308 and 323 K, as the pressure was increased from 2.5 to 4.0 kpsia, the axial dispersion coefficient was increased by 18.3 and 19.0% respectively. The axial dispersion coefficient in a packed bed may be a combination of the effects of molecular diffusion and convection. If we assume that the molecular diffusion decreases with increasing pressure, as predicted by the Wilke-Chang equation, then the measured results in this study suggest that the contribution by the convection is more important than the molecular diffusion under supercritical operating conditions. At 2.5, 3.2 and 4.0 kpsia, the axial dispersion coefficient was decreased by 17.7, 15.5 and 13.0% respectively, as the temperature of the extracting fluid was increased from 298 to 323 K. This dependence is again opposite to that of the molecular diffusion. Hence, the molecular diffusion might not play an important role for the axial dispersion coefficient as compared with the convection. Table 1 lists the density and viscosity of carbon dioxide at different operating temperatures and pressures. Since the mole fraction of hexachlorobenzene in carbon

dioxide was quite small, the density and viscosity of the carbon dioxide and hexachlorobenzene mixture could be regarded the same as those of the pure carbon dioxide. From Table 1 and Figure 3, it can be seen that the axial dispersion coefficient increases with an increase in density and viscosity of carbon dioxide. The viscosity of carbon dioxide was calculated using Thodos et al.[30] correlation.

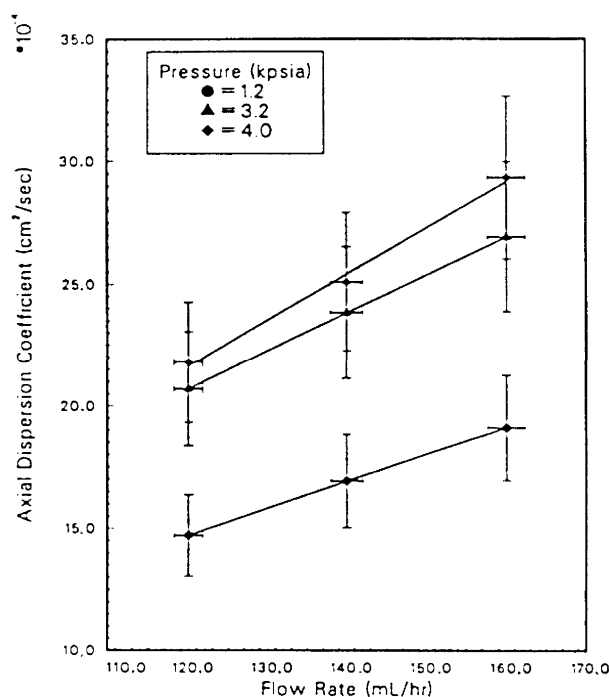


Figure 4. The effect of carbon dioxide flow rate on the axial dispersion coefficient at 298 K.

TABLE 2. The Comparison of the Experimental Peclet Number With the Empirical Correlation Values at Different Operating Temperatures and Pressures.

(P,kpsia)	298 K		308 K		323 K	
	Exp.	Correlation	Exp.	Correlation	Exp.	Correlation
1.2	0.403	0.430	—	—	—	—
1.7	0.470	0.441	—	—	—	—
2.5	0.520	0.446	0.443	0.473	0.436	0.432
3.2	0.568	0.450	0.445	0.529	0.441	0.480
4.0	0.613	0.452	0.450	0.580	0.445	0.533

$\frac{1}{\text{pec}\bar{A}}$  is Listed for Experimental and Empirical Correlation.

### B. FLOW RATE EXPERIMENTS

The next set of experiments investigated how the axial dispersion coefficient was influenced by the flow rate of the extracting fluid. Two series of experiments were conducted in this step. The first series of experiments was carried out at a constant temperature of 298 K. At three different operating pressures of 1.2, 3.2 and 4.0 kpsia, the axial dispersion coefficient was measured at three different flow rates of 120, 140 and 160 mL/hr. Figure 4 shows that the axial dispersion coefficient increases with increasing flow rate. For gases and liquids, the increase of axial dispersion coefficient with flow rate was also observed [12,31,32]. The second series of experiments was carried out at a system temperature of 323 K. The axial dispersion coefficient was measured at two different operating pressures of 3.2 and 4.0 kpsia. Figure 5 shows that the axial dispersion coefficient again increases with increasing flow rate at 323 K. The operating flow rates for this series of experiments were 120, 140 and 160 mL/hr.

If the Peclet number ( $\text{pec}\bar{A}$ ) for the packed bed is defined as  $u d_p / D_z$ , it is reported in the literature that it is usually less than 2.0 for liquids and greater than 2.0 for gases [22,31-33]. The measurements in this study showed that the

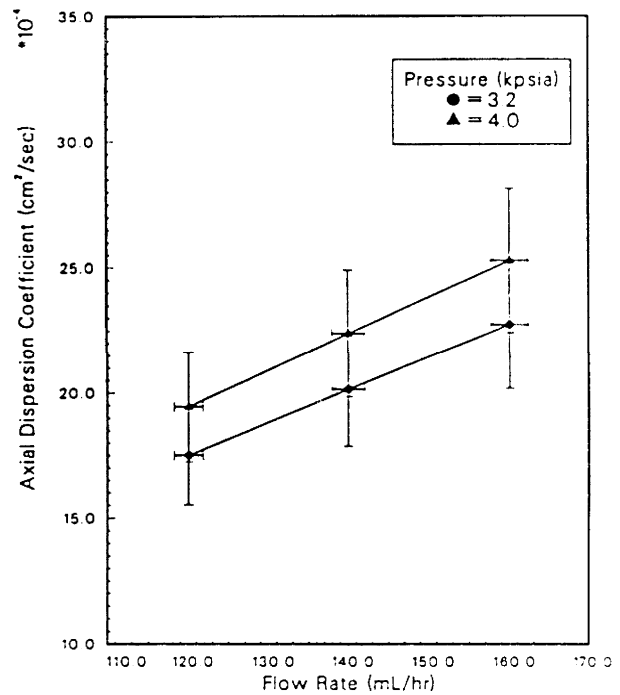
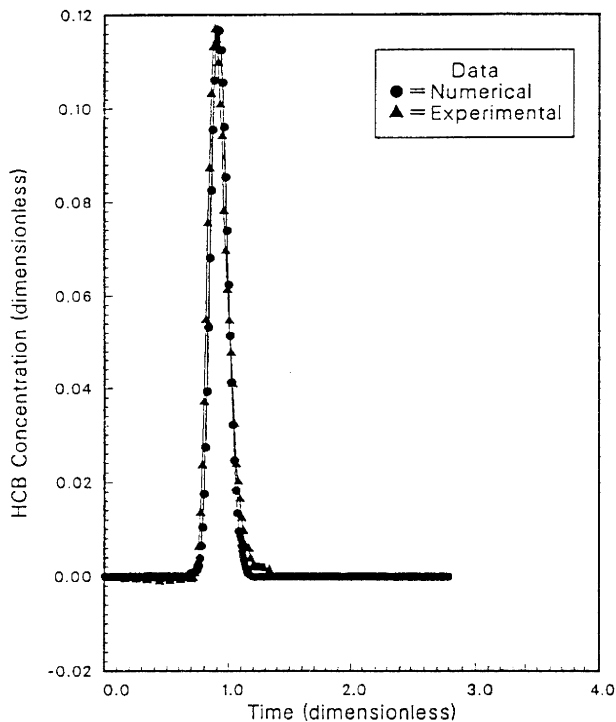


Figure 5. The effect of carbon dioxide flow rate on the axial dispersion coefficient at 323 K.

Peclet number lies between 1.50 and 2.50 for all combinations of operating variables. Since it has been realized that the behavior of a supercritical fluid lies between those of a gas and a liquid, the measured values in this study seem reasonable.

Yang [34] reported an empirical correlation for the axial dispersion coefficient in



**Figure 6.** The comparison of the numerical and experimental response peaks to a pulse input of HCB/CO<sub>2</sub> mixture for the glass beads experiments at 1.2 kpsia, 298 K and 160 mL/hr.

packedbeds. In this correlation, the Peclet number is correlated with

$$\frac{1}{\text{pec}\dot{A}} = \frac{0.3}{\text{Re Sc}} + \frac{0.5}{1+3.8/(\text{Re Sc})} \quad (31)$$

where

$$\text{Re} = \frac{r u d_p}{m} \quad \text{and} \quad \text{Sc} = \frac{m}{r D_m}$$

Reynolds and Schmidt numbers. This correlation is valid for  $0.008 < \text{Re} < 400$  and  $0.28 < \text{Sc} < 2.2$  and is capable of describing a peak in Peclet number and the asymptotic value of 2 for Peclet number at high Reynolds number. The diffusion coefficient ( $D_m$ ) of HCB in supercritical carbon dioxide is calculated by using the following equation developed by Rosset et al.[35]:

$$D_m = \frac{(8.6/10^{15}) (T M_s^{0.5})}{(m V^{0.6})} \quad (32)$$

Where  $T$  is the temperature in Kelvin,  $M_s$  is

the molecular weight (g) of the solvent,  $\mu$  is the solvent viscosity (Pa.sec) and  $V$  is the molar volume of the solvent at ambient temperature and pressure. Table 2 shows the Peclet number experimental values compared to those obtained from the empirical correlation. Even though the above correlation was not developed for the supercritical conditions and the required Schmidt number range was not satisfied, the deviation between the experimental and empirical values seems reasonable. The deviation between the two values increases at higher pressures which may be explained by considering the change in the value of Schmidt number (Table 3). The above correlation can be satisfied if the Schmidt number varies the range of 0.28 and 2.2. But the values for the Schmidt number in Table 3 show that we are operating outside the required range and this deviation increases with increasing pressure. For instance, at 298 K, the experimental Peclet number deviates from the correlation value at 1.2 (Sc= 3.34) and 4.0 kpsia (Sc= 5.8) by 6.3 and 26.3% respectively. Table 3 also shows that the diffusion coefficient decreases with increasing pressure and increases with increasing temperature. Figure 6 shows the numerical response peak and the experimental response curve for the glass beads experiments. The numerical response curve was obtained by solving the HCB mass balance differential equation. The small deviation between the two curves is well within the experimental error of axial dispersion coefficient measurements.

## CONCLUSIONS

The axial dispersion coefficients of supercritical carbon dioxide were measured in a fixed-bed packed with glass beads using the on-line chromatographic pulse-response experiment.

TABLE 3. The Diffusion Coefficient and the Schmidt Number at Different Operating Temperatures and Pressures.

(P, kpsia)	298 K		308 K		323 K	
	$D_m$	Sc	$D_m$	Sc	$D_m$	Sc
1.2	0.2408	3.34	—	—	—	—
1.7	0.2083	4.10	—	—	—	—
2.5	0.1888	4.74	0.2019	4.56	0.2290	4.10
3.2	0.1744	5.36	0.1890	4.88	0.2099	4.60
4.0	0.1656	5.80	0.1730	5.65	0.1915	5.19

$D_m = [\text{cm}^2/\text{sec}] [10^3]$

The range of the operating conditions for temperature, pressure and flow rate of supercritical fluid were 25-50°C, 1200-4000 psia and 120-160 mL/hr, respectively. The experimental data indicated that the axial dispersion coefficient is a function of temperature, pressure and flow rate of carbon dioxide. The axial dispersion coefficient decreased with increasing temperature and increased with increasing pressure. This trend may be due to the increase of the density and viscosity of the supercritical carbon dioxide. Furthermore, the axial dispersion coefficient increased with increasing interstitial velocity. This result may suggest that the contribution by convection is more important than that of molecular diffusion under supercritical operations. Much work needs to be done in order to correlate the dependence of the axial dispersion upon the fluid physical properties, operation variables and the packed column geometry applicable for supercritical fluids.

#### ACKNOWLEDGMENT

**Credits.** Financial support for this project by the Captiva Inc. (USA) is gratefully acknowledged.

**Authors.** Dr. Seyyed Mohammad Ghoreishi (B.S., 1984, University of Texas at Austin;

Ph.D., 1990, Texas A&M University, USA) is assistant professor in the Department of Chemical Engineering at Isfahan University of Technology. Dr. Aydin Akgerman (Ph.D., 1971, University of Virginia, USA) is professor in the Department of Chemical Engineering at Texas A&M University.

#### NOTATION

$A_C$	Packed column cross sectional area, $\text{cm}^2$
$C_A$	Concentration of solute in the mobile phase, $\text{g}/\text{cm}^3$
$C_{A_0}$	Concentration of solute in the influent, $\text{g}/\text{cm}^3$
$C_A^*$	Laplace transformation of $C_A$
$C_A^{**}$	dimensionless variable, $C_A/C_{A_0}$
$d_p$	diameter of spherical particle, cm
$D_Z$	axial dispersion coefficient, $\text{cm}^2/\text{sec}$
$D_m$	diffusion coefficient, $\text{cm}^2/\text{sec}$
$F$	arbitrary function
$L$	length of the extraction column, cm
$M_s$	molecular weight of the solvent, g
$Pec$	Peclet number, dimensionless, $uL/D_Z$
$Pec_A$	Peclet number, dimensionless, $ud_p/D_Z$
$Q$	volumetric flow rate, mL/hr
$Re$	Reynolds number, dimensionless, $rud_p/m$
$s$	Laplace transformation variable
$Sc$	Schmidt number, dimensionless, $m/rD_m$
$t$	time, sec
$T$	temperature, k
$u$	interstitial velocity, $\text{cm}/\text{sec}$ , $Q/A_c \epsilon_z$
$V$	molar volume, $\text{cm}^3/\text{mol}$
$X$	axial dimensionless variable, $Z/L$
$Z$	axial dimension of the packed bed, cm

## Greek Letters

$t$	injection time of the square pulse input, sec
$\epsilon(x)$	experimental error in the quantity $x$
$j$	equal to $L/u$ , sec
$\epsilon_z$	void fraction of the packed bed
$q$	dimensionless variable, $t/j$
$\rho$	density, $g/cm^3$
$\mu$	viscosity, $g/cm.sec$ , $Pa.sec$
$\mu_0$	zeroth reduced moment
$\mu_1$	first absolute moment, sec
$\mu_2$	second absolute moment, $sec^2$
$\mu_A$	second central moment, $sec^2$

## LITERATURE CITED

1. Madras, G., Erkey, C. and Akgerman, A., "A New Technique for Measuring Solubilities of Organics in Supercritical Fluids", *J. Chem. Eng. Data*, 38, 422, (1993a).
2. Dooley, K. M., Kao, C. P., Gambrell, R. P. and Knopf, F. C., "The Use of Entrainers in the Supercritical Extraction of Soils Contaminated with Hazardous Organics", *Ind. Eng. Chem. Res.*, 26, 2058, (1987).
3. Roop, R. K., Hess R. K. and Akgerman, A., "Supercritical Extraction of Priority Pollutants from Water and Soil", *Supercritical Fluid Science and Technology*, K. P. Johnston and J. M. L. Penniger, Eds., Amer. Chem. Soc., Washington, DC, (1989).
4. Erkey, C., Madras, G., Orejuela M. and Akgerman, A., "Supercritical Fluid Extraction of Polyaromatic Hydrocarbons Combined with Adsorption onto Activated Carbon", *Environ. Sci. Technol.*, 27, 1225, (1993).
5. Foster N. R. and Macnaughton, S. J., "Supercritical Adsorption and Desorption Behavior of DDT on Activated Carbon Using Carbon Dioxide", *Ind. Eng. Chem. Res.*, 34, 275, (1995).
6. Madras, G., Thibaud, C., Erkey, C. and Akgerman, A., "Modeling of Supercritical Extraction of Organics from Solid Matrices", *AIChE Journal* 40, 40777, (1994).
7. Zhou, L., Erkey C. and Akgerman, A., "Catalytic Oxidation of Toluene and Tetralin in Supercritical Carbon Dioxide", *AIChE Journal* 41, 2122, (1995).
8. Simoes, P. C., Matos, H. A., Carmelo, P. J., DeAzevedo E. G. and Da Ponte, M. N., "Mass Transfer in Countercurrent Packed Columns: Application to Supercritical CO<sub>2</sub> Extraction of Terpenes", *Ind. Eng. Chem. Res.*, 34, 613, (1995).
9. Zhou, L. and Akgerman, A., "Catalytic Oxidation of Ethanol and Acetaldehyde in Supercritical Carbon Dioxide", *Ind. Eng. Chem. Res.*, 34, 1588, (1995).
10. Levenspiel O. and Smith, W. K., "Notes on the Diffusion-Type Model for the Longitudinal Mixing of Fluids in Flow", *Chem. Eng. Sci.*, 6, 227, (1957).
11. Danckwerts, P. V., "Continuous Flow Systems, Distribution of Residence Times", *Chem. Eng. Sci.*, 2, 1, (1953).
12. Liles A. W. and Geankoplis, C. J., "Axial Diffusion of Liquids in Packed Beds and End Effects", *AIChE Journal* 6, 591, (1960).
13. Miller S. F. and King, C. J., "Axial Dispersion in Liquid Flow Through Packed Beds", *AIChE Journal*, 12, 767, (1966).
14. Schneider, P. and Smith, J. M., "Adsorption Rate Constants from Chromatography" , *AIChE Journal* 14, 762, (1968).
15. Gunn, D. J., "The Transient and Frequency Response of Particles and Beds of Particles", *Chem. Eng. Sci.*, 25, 53, (1970).
16. Suzuki, M. and Smith, J. M., "Kinetic Studies by Chromatography", *Chem. Eng. Sci.*, 26, 221, (1971).
17. Wakao, N., Lida, Y. and Tanisho, S., "Determination of Fluid Dispersion Coefficients in Packed Beds", *J. Chem. Eng. Japan*, 7, 438, (1974).
18. Furusawa, T., Suzuki, M. and Smith, J. M., "Rate Parameters in Heterogeneous Catalysis by Pulse Techniques", *Catal. Rev. Sci. Eng.*, 13 (1), 43, (1976).
19. Kubo, K., Aratani, T., Mishima, A. and Yano, T., "Identification of Axial Liquid Mixing Models for Packed Beds", *Journal Chem. Eng. Japan*, 11, (1978)234.
20. Parulekar S. J. and Ramkrishna, D., "Analysis of Axially Dispersed Systems with General Boundary Conditions-"I, II, III", *Chem. Eng. Sci.*, 39, 1571, (1984).
21. Hill, C. G., "Chemical Engineering Kinetics and Reactor Design", J. Wiley, New York (1979).
21. Han, N. W., Bhakta, J. and Carbonell, R. G., "Longitudinal and Lateral Dispersion in Packed Beds: Effect of Column Length and Particle Size Distribution", *AIChE Journal* 31, 277, (1985).
22. Gunn, D. J., "Axial and Radial Dispersion in Fixed Beds", *Chem. Eng. Sci.*, 42, 363, (1987).
23. Lee, W., Huang, S. H. and Tsao, G. T., "A Unified Approach for Moments in Chromatography", *AIChE Journal* 34, 2083, (1988).
24. Westerterp, K. R., Dilman, V. V. and Kronberg, A. E.,

- "Wave Model for Longitudinal Dispersion: Development of the Model", *AIChE Journal*, 41, (2013), (1995).
25. Moore, C. M. V. and Cooney, C. L., "Axial Dispersion in Taylor-Couette Flow", *AIChE Journal*, 41, 723, (1995).
26. Kohay, T., Richardson, J. T. and Luoss, D., "Axial Dispersion of Solid Particles in a Continuous Rotary Kiln", *AIChE Journal*, 41, 2465, (1995).
27. Tan, C. and Liou, D., "Axial Dispersion of Supercritical Carbon Dioxide in Packed Beds", *Ind. Eng. Chem. Res.*, 28, 1246, (1989).
28. Lee, C. H. and Holder, G. D., "Use of Supercritical Fluid Chromatography for Obtaining Mass Transfer Coefficients in Fluid-Solid Systems at Supercritical Conditions", *Ind. Eng. Chem. Res.*, 34, 906, (1995).
29. Ruthven, D. M., "Principles of Adsorption and Adsorption Processes", J. Wiley, New York, (1984).
30. Thodos, G., Jossi J. A. and Stiel, L. I., "Viscosity of Nonpolar Gases", *AIChE Journal*, 8, 59, (1962).
31. Ebach, E. A. and White, R. R., "Mixing of Fluids Flowing Through Beds of Packed Solids", *AIChE Journal*, 4, 161, (1958).
32. Fu, C. C., Ramesh, M. S. P. and Haynes, H. W., "Analysis of Gas Chromatography Pulse Dispersion Data for the System n-Butane/Zeolite", *AIChE Journal*, 32, 1848, (1986).
34. Yang, R. T., "Gas Separation by Adsorption Processes", Butterworths, Ma (1987).
35. Rosset, R. H., Sassi, P. R., Mourier, P. and Caude, M. H., "Measurement of Diffusion Coefficients in Supercritical Carbon Dioxide and Correlation with the Equation of Wilke and Chang", *Amer. Chem. Soci.*, 55, (1987)1375.